

## Very Large Difference in Electronic Communication of Dimetal Species with Heterobiphenylene and Heteroanthracene Units

F. Albert Cotton,<sup>†</sup> Carlos A. Murillo,\* Mark D. Young, Rongmin Yu, and Qinliang Zhao

Department of Chemistry and Laboratory for Molecular Structure and Bonding, P.O. Box 30012, Texas A&M University, College Station, Texas 77842-3012

Received September 29, 2007

Two neutral compounds having [Mo<sub>2</sub>] units linked by squarate dianions, [Mo<sub>2</sub>(DAniF)<sub>3</sub>]<sub>2</sub>(μ<sub>4</sub>-C<sub>4</sub>O<sub>4</sub>) (DAniF = *N,N'*-di(*p*-anisyl)formamidinate) (**1**) and [Mo<sub>2</sub>(DmCF<sub>3</sub>F)<sub>3</sub>]<sub>2</sub>(μ<sub>4</sub>-C<sub>4</sub>O<sub>4</sub>) (DmCF<sub>3</sub>F = *N,N'*-di(*m*-trifluoromethylphenyl)formamidinate) (**2**), as well as the singly oxidized compound {[Mo<sub>2</sub>(DmCF<sub>3</sub>F)<sub>3</sub>]<sub>2</sub>(μ<sub>4</sub>-C<sub>4</sub>O<sub>4</sub>)}SbF<sub>6</sub> (**3**) and the doubly oxidized species {[Mo<sub>2</sub>(DAniF)<sub>3</sub>]<sub>2</sub>(μ<sub>4</sub>-C<sub>4</sub>O<sub>4</sub>)}(TFPB)<sub>2</sub> (TFPB = [B(3,5-(CF<sub>3</sub>)<sub>2</sub>C<sub>6</sub>H<sub>3</sub>)<sub>4</sub>]<sup>-</sup>) (**4**), were synthesized and structurally characterized. Electrochemical measurements of the two neutral species showed only very weak electronic interactions between the two dimolybdenum units linked by the squarate anion in contrast to what was observed in dioxolene analogues having C<sub>6</sub> instead of C<sub>4</sub> rings (*J. Am. Chem. Soc.* **2006**, *128*, 3281) which led to differences in comproportionation constants of over 10<sup>8</sup>. In the squarate species, the π electrons are localized within the carbonyl and dimetal units in the heterometallic six-membered Mo<sub>2</sub>O<sub>2</sub>C<sub>2</sub> rings to minimize the antiaromaticity in the central C<sub>4</sub> square. The oxidized species **3** and **4** are electronically localized in the time scale of the physical measurements. Calculations at the DFT level suggested that the energy mismatch of the frontier orbitals of the linker and dimetal units contributes to the weak communication between the Mo<sub>2</sub> units. For the doubly oxidized complex **4**, DFT calculations gave a *J* value of -130 cm<sup>-1</sup> which suggests that the two unpaired electrons are only weakly antiferromagnetically coupled, as shown by magnetic studies (*J* = -121 cm<sup>-1</sup>).

### Introduction

The study of electronic interactions between redox centers mediated by extended, polyfunctional bridging groups has been a topic of great interest for decades in inorganic and bioinorganic chemistry.<sup>1</sup> After the pioneering work on the Creutz–Taube ion,<sup>2</sup> which has two ruthenium ions in different oxidation states linked by a neutral pyrazine linker, major efforts have been made toward the preparation of other mixed-valence analogues and the study of their properties.<sup>3</sup> An important goal has been to understand the nature of such

interactions which are of fundamental importance in biological systems and the design of new materials.<sup>3</sup>

Electronic interactions between two redox centers have been investigated with various linkers.<sup>4</sup> In our laboratory, as well as Chisholm's,<sup>5</sup> we have extended the study of electronic interactions between redox centers to include dimolybdenum units such as Mo<sub>2</sub>(DAniF)<sub>3</sub><sup>+</sup> (DAniF = *N,N'*-di(*p*-anisyl)formamidinate), which will be abbreviated as [Mo<sub>2</sub>]. Pairs of [Mo<sub>2</sub>] units give the so-called *dimers of dimers* (or pairs) with a variety of linkers.<sup>6–12</sup> It has been

\* To whom correspondence should be addressed. E-mail: murillo@tamu.edu.

<sup>†</sup> Deceased, February 20, 2007.

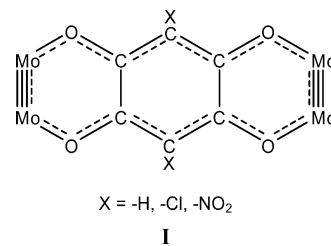
- (1) See for example: (a) Creutz, C. *Prog. Inorg. Chem.* **1983**, *30*, 1. (b) Richardson, D. E.; Taube, H. *Coord. Chem. Rev.* **1984**, *60*, 107. (c) Chen, P.; Meyer, T. J. *Chem. Rev.* **1998**, *98*, 1439. (d) Ferretti, A.; Lami, A.; Murga, L. F.; Shehadi, I. A.; Ondrechen, M. J.; Villani, G. *J. Am. Chem. Soc.* **1999**, *121*, 2594. (e) Kaim, W.; Klein, A.; Gloeckle, M. *Acc. Chem. Res.* **2000**, *33*, 755. (f) Demadis, K. D.; Hartshorn, C. M.; Meyer, T. J. *Chem. Rev.* **2001**, *101*, 2655. (g) Brunshwig, B. S.; Creutz, C.; Sutin, N. *Chem. Soc. Rev.* **2002**, *31*, 168. (h) Lau, V. C.; Berben, L. A.; Long, J. R. *J. Am. Chem. Soc.* **2002**, *124*, 9042. (2) (a) Creutz, C.; Taube, H. *J. Am. Chem. Soc.* **1969**, *91*, 3988. (b) Creutz, C.; Taube, H. *J. Am. Chem. Soc.* **1973**, *95*, 1086.

- (3) See for example: (a) Prassides, K., Ed. *Mixed-valency Systems: Applications in Chemistry, Physics and Biology*; Kluwer Academic Publishers: Dordrecht, 1991. (b) Cembran, A.; Bernardi, F.; Olivucci, M.; Garavelli, M. *Proc. Nat. Acad. Sci. U.S.A.* **2005**, *102*, 6255. (c) Talukdar, P.; Bollot, G.; Mareda, J.; Sakai, N.; Matile, S. *J. Am. Chem. Soc.* **2005**, *127*, 6528. (d) Fiedler, A. T.; Bryngelson, P. A.; Maroney, M. J.; Brunold, T. C. *J. Am. Chem. Soc.* **2005**, *127*, 5449. (e) Sakharov, D. V.; Lim, C. *J. Am. Chem. Soc.* **2005**, *127*, 4921. (f) Efimov, I.; McIntire, W. S. *J. Am. Chem. Soc.* **2005**, *127*, 732. (g) O'Neill, M. A.; Dohno, C.; Barton, J. K. *J. Am. Chem. Soc.* **2004**, *126*, 1316. (h) Lewis, F. D.; Wu, Y.; Zhang, L.; Zuo, X.; Gayes, R. T.; Wasielewski, M. R. *J. Am. Chem. Soc.* **2004**, *126*, 8206. (i) Wan, C.; Fiebig, T.; Schiemann, O.; Barton, J. K.; Zewail, A. H. *Proc. Nat. Acad. Sci. U.S.A.* **2000**, *97*, 14052. (j) Hess, S.; Götz, M.; Davis, W. B.; Michel-Beyerle, M. E. *J. Am. Chem. Soc.* **2001**, *123*, 10046.

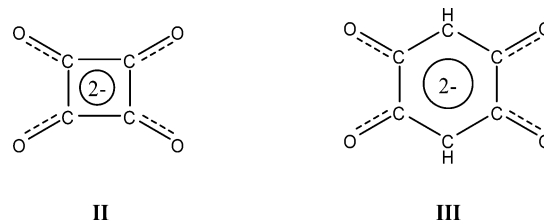
shown that with appropriate modifications to the linker the electronic interactions between dimetal units may be modulated to a large extent.<sup>5</sup>

We recently reported unprecedented and very strong electronic communication in dimolybdenum pairs linked by dioxolene anions  $C_6X_2O_4^{2-}$  ( $X = H, Cl, \text{ or } NO_2$ ) (**I** in Scheme 1)<sup>13</sup> and in the N-substituted benzoquinonemonoimine analogues.<sup>14,15</sup> In these compounds, with core structures resembling heteroanthracenes, strong  $\pi$  interactions between  $\delta$  orbitals from the  $[Mo_2(DAniF)_3]^+$  units and p orbitals from the linker favor electron delocalization that extends through the periphery of the core including the linker

Scheme 1



Scheme 2



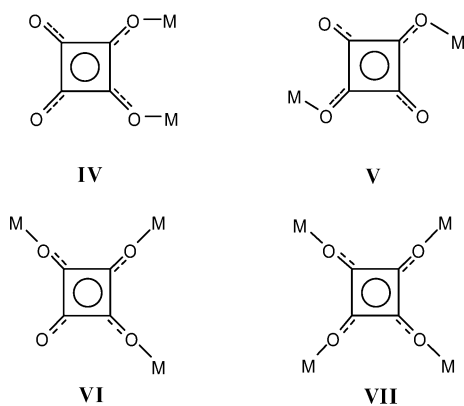
and the four Mo atoms, as shown by broken lines in Scheme 1. In this case participation of  $\delta$  orbitals of the dimetal units is necessary. This pathway for electron delocalization is unique to systems with quadruply bonded dimetal units as such pathway is clearly unavailable for single metal species such as the Creutz–Taube ion and its analogues.<sup>16</sup>

The squarate dianion (**II** in Scheme 2) can be viewed as a dioxolene analogue (**III**) in which the  $C_6$  ring has been replaced by a  $C_4$  ring. To the best of our knowledge, the squarate dianion has never been used as a bis-bidentate linker in mixed-valence dinuclear complexes, even though it is known to give a variety of binding modes<sup>17,18</sup> such as those shown in Scheme 3.<sup>19</sup> It has also been pointed out that the squarate ligand does not generally act as a bis-bidentate linker in first-row transition-metal complexes because of its very large bite angle relative to that of the oxalate dianion (*b* in Scheme 4).<sup>20</sup> Here, we report the preparation and characterization of the neutral compounds  $[Mo_2(DAniF)_3]_2(\mu_4-C_4O_4)$  (**1**) and  $[Mo_2(DmCF_3F)_3]_2(\mu_4-C_4O_4)$ , ( $DmCF_3F = N,N'$ -di-(*m*-trifluoromethylphenyl)formamidinate) (**2**), as well as the singly oxidized compound  $\{[Mo_2(DmCF_3F)_3]_2(\mu_4-C_4O_4)\}^-$

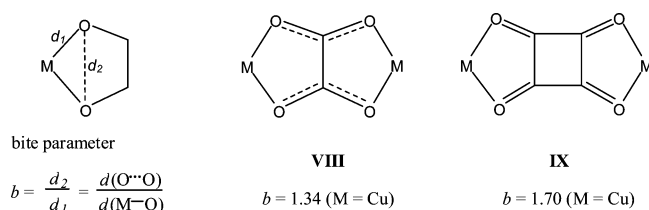
- (4) (a) Harding, C.; McDowell, D.; Nelson, J.; Raghunathan, S.; Stevenson, C.; Drew, M. G. B.; Yates, P. C. *J. Chem. Soc., Dalton Trans.* **1990**, 2521. (b) Hodgson, D. J. *J. Mol. Catal.* **1984**, *23*, 219. (c) Mazurek, W.; Berry, K. J.; Murray, K. S.; O'Connor, M. J.; Snow, M. R.; Wedd, A. G. *Inorg. Chem.* **1982**, *21*, 3071. (d) Shoji, O.; Okada, S.; Satake, A.; Kobuke, Y. *J. Am. Chem. Soc.* **2005**, *127*, 2201. (e) Davis, A. R.; Einstein, F. W. B. *Inorg. Chem.* **1980**, *19*, 1203. (f) Lucas, N. T.; Notaras, E. G. A.; Petrie, S.; Stranger, R.; Humphrey, M. G. *Organometallics* **2003**, *22*, 708. (g) Kurreck, H.; Huber, M. *Angew. Chem., Int. Ed. Engl.* **1995**, *34*, 849. (h) Launay, J.-P. *Chem. Soc. Rev.* **2001**, *30*, 386. (i) Ortega, J. V.; Hong, B.; Ghosal, S.; Hemminger, J. C.; Breedlove, B.; Kubiak, C. P. *Inorg. Chem.* **1999**, *38*, 5102. (j) Hong, B.; Woodcock, S. R.; Saito, S. K.; Ortega, J. V. *J. Chem. Soc., Dalton Trans.* **1998**, 2615. (k) Valentin, M. D.; Bisol, A.; Agostini, G.; Carbonera, D. *J. Chem. Inf. Model.* **2005**, *45*, 1580. (l) Liddell, P. A.; Kuciauskas, D.; Sumida, J. P.; Nash, B.; Nguyen, D.; Moore, A. L.; Moore, T. A.; Gust, D. *J. Am. Chem. Soc.* **1997**, *119*, 1400. (m) Ribou, A.-C.; Launay, J.-P.; Takahashi, K.; Nihira, T.; Tarutani, S.; Spangler, C. W. *Inorg. Chem.* **1994**, *33*, 1325. (n) Siri, O.; Taquet, J.-P.; Collin, J.-P.; Rohmer, M.-M.; Bénard, M.; Braunstein, P. *Chem. Eur. J.* **2005**, *11*, 7247. (o) Siri, O.; Braunstein, P.; Taquet, J.-P.; Collin, J.-P.; Welter, R. *Dalton Trans.* **2007**, 1481.
- (5) (a) Cotton, F. A.; Lin, C.; Murillo, C. A. *Acc. Chem. Res.* **2001**, *34*, 759. (b) Cotton, F. A.; Lin, C.; Murillo, C. A. *Proc. Nat. Acad. Sci. U.S.A.* **2002**, *99*, 4810. (c) Cotton, F. A.; Liu, C. Y.; Murillo, C. A.; Wang, X. *Chem. Commun.* **2003**, 2190. (d) Cotton, F. A.; Donahue, J. P.; Huang, P.; Murillo, C. A.; Villagrán, D. *Z. Anorg. Allg. Chem.* **2005**, *631*, 2606. (e) Cotton, F. A.; Donahue, J. P.; Murillo, C. A. *Inorg. Chem. Commun.* **2002**, *5*, 59. (f) Cotton, F. A.; Daniels, L. M.; Donahue, J. P.; Liu, C. Y.; Murillo, C. A. *Inorg. Chem.* **2002**, *41*, 1354. (g) Chisholm, M. H. *Proc. Nat. Acad. Sci. U.S.A.* **2007**, *104*, 2563. (h) Chisholm, M. H.; Macintosh, A. M. *Chem. Rev.* **2005**, *105*, 2949. (i) Chisholm, M. H.; Patmore, N. *J. Acc. Chem. Res.* **2007**, *40*, 19.
- (6) (a) Cotton, F. A.; Dalal, N. S.; Liu, C. Y.; Murillo, C. A.; North, J. M.; Wang, X. *J. Am. Chem. Soc.* **2003**, *125*, 12945. (b) Cotton, F. A.; Donahue, J. P.; Murillo, C. A. *Inorg. Chem.* **2001**, *40*, 2229.
- (7) Cotton, F. A.; Liu, C. Y.; Murillo, C. A.; Wang, X. *Inorg. Chem.* **2003**, *42*, 4619.
- (8) (a) Cotton, F. A.; Donahue, J. P.; Lin, C.; Murillo, C. A. *Inorg. Chem.* **2001**, *40*, 1234. (b) Cotton, F. A.; Donahue, J. P.; Murillo, C. A. *J. Am. Chem. Soc.* **2003**, *125*, 5436. (c) Cotton, F. A.; Donahue, J. P.; Murillo, C. A.; Pérez, L. M. *J. Am. Chem. Soc.* **2003**, *125*, 5486.
- (9) Cotton, F. A.; Li, Z.; Liu, C. Y.; Murillo, C. A. *Inorg. Chem.* **2006**, *45*, 9765.
- (10) Cotton, F. A.; Liu, C. Y.; Murillo, C. A.; Villagrán, D.; Wang, X. *J. Am. Chem. Soc.* **2004**, *126*, 14822.
- (11) (a) Cotton, F. A.; Liu, C. Y.; Murillo, C. A.; Villagrán, D.; Wang, X. *J. Am. Chem. Soc.* **2003**, *125*, 13564. (b) Cotton, F. A.; Liu, C. Y.; Murillo, C. A.; Zhao, Q. *Inorg. Chem.* **2007**, *46*, 2604.
- (12) Cotton, F. A.; Donahue, J. P.; Murillo, C. A.; Pérez, L. M.; Yu, R. *J. Am. Chem. Soc.* **2003**, *125*, 8900.
- (13) Cotton, F. A.; Murillo, C. A.; Villagrán, D.; Yu, R. *J. Am. Chem. Soc.* **2006**, *128*, 3281.
- (14) Cotton, F. A.; Jin, J.-Y.; Li, Z.; Murillo, C. A.; Reibenspies, J. H. *Chem. Commun.* **2007**, in press.
- (15) It should be noted that benzoquinonemonoimine species with single metal units were first made by Braunstein et al. and have attracted great attention because they are antiaromatic, having  $6\pi + 6\pi$  electrons. For example, see: (a) Siri, O.; Braunstein, P.; Rohmer, M.-M.; Bénard, M. *R. J. Am. Chem. Soc.* **2003**, *125*, 13793. (b) Yang, Q.-Z.; Siri, O.; Braunstein, P. *Chem. Commun.* **2005**, 2660. (c) Siri, O.; Braunstein, P. *Chem. Commun.* **2000**, 2223.

- (16) For example, see work on nickel and copper complexes reported in the 1970s: Pierpont, C. G.; Francesconi, L. C.; Hendrickson, D. N. *Inorg. Chem.* **1977**, *16*, 2367.
- (17) (a) Brouca-Cabarrecq, C.; Mohanu, A.; Millet, P.; Trombe, J. C. *J. Solid State Chem.* **2004**, *177*, 2575. (b) Modéc, B.; Brenèdiè, J. V.; Burkholder, E. M.; Zubieta, J. *Dalton Trans.* **2003**, 4618. (c) Lai, S. F.; Cheng, C.-Y.; Lin, K. J. *Chem. Commun.* **2001**, 1082. (d) Krupicka, E.; Lentz, A.; Kristallog, Z. *New Cryst. Struct.* **2001**, *216*, 289. (e) Fabre, P. L.; Galibert, A. M.; Soula, B.; Dahan, F.; Castan, P. *Dalton Trans.* **2001**, 1529. (f) Crispini, A.; Pucci, D.; Aiello, I.; Ghedini, M. *Inorg. Chim. Acta* **2000**, *304*, 219. (g) Castro, I.; Calatayud, M. L.; Sletten, J.; Lloret, F.; Julve, M. *J. Chem. Soc., Dalton Trans.* **1997**, 811. (h) Castro, I.; Calatayud, M. L.; Sletten, J.; Lloret, F.; Julve, M. *Inorg. Chim. Acta* **1999**, 287, 173.
- (18) (a) Thrombe, J. C.; Petit, J. F.; Gleizes, A. *Inorg. Chim. Acta* **1990**, *167*, 69. (b) Robl, C.; Weiss, A. *Mater. Res. Bull.* **1987**, *22*, 373. (c) Calatayud, M. L.; Castro, I.; Sletten, J.; Cano, J.; Lloret, F.; Faus, J.; Julve, M.; Seitz, G.; Mann, K. *Inorg. Chem.* **1996**, *35*, 2858.
- (19) There have been suggestions that this ligand may potentially bind to transition metal ions as a bis-bidentate linker, and at least a magnetic study has been reported on a nickel species that has been claimed to be a dinuclear species. However, it should be noted that this compound has not been structurally characterized. See: Duggan, D. M.; Barefield, E. K.; Hendrickson, D. N. *Inorg. Chem.* **1973**, *12*, 985.
- (20) (a) Solans, X.; Aguilü, M.; Gleizes, A.; Faus, J.; Julve, M. *Inorg. Chem.* **1990**, *29*, 775. (b) Kepert, D. L. *Prog. Inorg. Chem.* **1977**, *23*, 1.

## Scheme 3



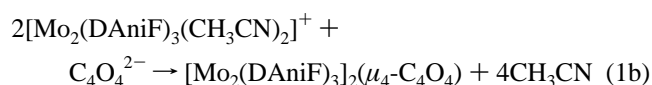
## Scheme 4



SbF<sub>6</sub> (**3**) and the doubly oxidized species {[Mo<sub>2</sub>(DAniF)<sub>3</sub>]<sub>2</sub>-(μ<sub>4</sub>-C<sub>4</sub>O<sub>4</sub>)}(TFPB)<sub>2</sub> (TFPB = [B(3,5-(CF<sub>3</sub>)<sub>2</sub>C<sub>6</sub>H<sub>3</sub>)<sub>4</sub>]<sup>-</sup>) (**4**). The doubly oxidized species **4** represents the only example of a dimer of dimers having two weakly coupled dimetal units that has been isolated and fully characterized.

## Results and Discussion

**Syntheses.** Compound **1** was prepared in a two-step process according to eqs 1a and 1b.

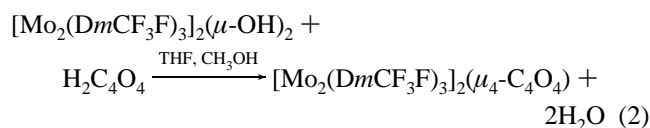


In step two, the neutral product precipitates from acetonitrile solutions as an orange microcrystalline solid that is conveniently isolated by filtration and then recrystallized by dissolving the product in CH<sub>2</sub>Cl<sub>2</sub> and adding a layer of diethyl ether. Compound **1** readily decomposes upon exposure to air.

Because electrochemical measurements (vide infra) suggested that **1** could potentially be oxidized by ferrocenium salts such as [Cp<sub>2</sub>Fe]X, X = BF<sub>4</sub> or PF<sub>6</sub>, to the corresponding singly and doubly oxidized species, these oxidizing agents were indeed used. However, the singly oxidized product was only slightly soluble in most common organic solvents such as CH<sub>2</sub>Cl<sub>2</sub>. With the idea of increasing the solubility of the singly oxidized species oxidation attempts were also carried out using [Cp<sub>2</sub>Fe]TFPB. Even though this procedure produced an oxidized species, crystallization of the reaction product always resulted in the isolation of red crystals composed of 1 equiv of the neutral species and two

equivalents of the singly oxidized compound.<sup>21</sup> If an excess of [Cp<sub>2</sub>Fe]TFPB was employed, further oxidation took place with formation of the stable doubly oxidized species **4**, which was easily crystallized from CH<sub>2</sub>Cl<sub>2</sub> solutions to which a layer of isomeric hexanes had been added. Compound **4** is soluble in many common organic solvents such as CH<sub>2</sub>Cl<sub>2</sub>, THF, CH<sub>3</sub>CN, C<sub>2</sub>H<sub>5</sub>OH, and diethyl ether.

To obtain a crystalline product composed entirely of the pure singly oxidized squarate-bridged species, another neutral dimolybdenum pair **2** was synthesized. Its preparation, summarized in eq 2, involved a new method using a recently reported molecular pair linked by two hydroxide groups, [Mo<sub>2</sub>(DmCF<sub>3</sub>F)<sub>3</sub>]<sub>2</sub>(μ-OH)<sub>2</sub>,<sup>22</sup> as starting material. The latter is readily prepared from Mo<sub>2</sub>(DmCF<sub>3</sub>F)<sub>3</sub>(OAc).<sup>22</sup>



This acid–base reaction appears to be a general method, but although neutralization reactions are generally fast, that in eq 2 requires a long reaction period because of the very low solubility of squaric acid. The target product was obtained in moderate yield. Crystals were obtained from CH<sub>2</sub>Cl<sub>2</sub> solutions of the product to which a layer of ethanol had been added.

The singly oxidized compound **3** was prepared at room temperature in CH<sub>2</sub>Cl<sub>2</sub> by reaction of the neutral species **2** with 1 equiv of NOSbF<sub>6</sub>. Similarly to the oxidized product of **1** obtained when using ferrocenium salts as oxidizing agents, compound **3** is also rather insoluble in CH<sub>2</sub>Cl<sub>2</sub>. However, in this case crystals formed directly from the reaction mixture if stirring was avoided during the reaction. It should be noted that attempts to recrystallize **3** by heating dichloromethane solutions led to decomposition.

**Structures.** The structures of **1** and **2**, shown in Figure 1, are closely related even though they have formamidate ligands with vastly different electron donating properties.<sup>23</sup> For the two compounds, bond distances and angles, as well as the core conformations are essentially identical. The squarate dianion links two [Mo<sub>2</sub>] units forming two six-membered Mo–Mo–O–C–C–O rings, fused together

(21) Crystal data for [Mo<sub>2</sub>(DAniF)<sub>3</sub>]<sub>2</sub>(C<sub>4</sub>O<sub>4</sub>)·2{[Mo<sub>2</sub>(DAniF)<sub>3</sub>]<sub>2</sub>(C<sub>4</sub>O<sub>4</sub>)}-(TFPB): triclinic, space group *P*1̄, *a* = 18.383(2) Å, *b* = 19.175(2) Å, *c* = 30.077(4) Å, α = 106.233(6)°, β = 96.206(7)°, γ = 109.366(7)°, *V* = 9365(2) Å<sup>3</sup>, *Z* = 1, *R* value [*I* > 2σ] *R*<sub>1</sub> = 0.138. In the asymmetric unit, there is a half moiety of the neutral compound **1** and an entire molecule of the singly oxidized compound {[Mo<sub>2</sub>(DAniF)<sub>3</sub>]<sub>2</sub>(C<sub>4</sub>O<sub>4</sub>)}(TFPB). The quality of the diffraction data for this crystal was insufficient for a detailed structural analysis. However, in the singly oxidized species, the analysis unambiguously shows the existence of molecular pairs composed of two [Mo<sub>2</sub>] units and a squarate dianion. The crystallographically independent [Mo<sub>2</sub>] units have different Mo–Mo bond distances, 2.110(3) and 2.148(3) Å, for the Mo<sub>2</sub><sup>4+</sup> unit and the oxidized Mo<sub>2</sub><sup>5+</sup> unit, respectively, indicating that the odd electron is localized on a single [Mo<sub>2</sub>] unit in the timescale of X-ray analysis.

(22) Cotton, F. A.; Murillo, C. A.; Yu, R.; Zhao, Q. *Inorg. Chem.* **2006**, *45*, 9046.

(23) Lin, C.; Protasiewicz, J. D.; Ren, T. *Inorg. Chem.* **1996**, *35*, 6422.



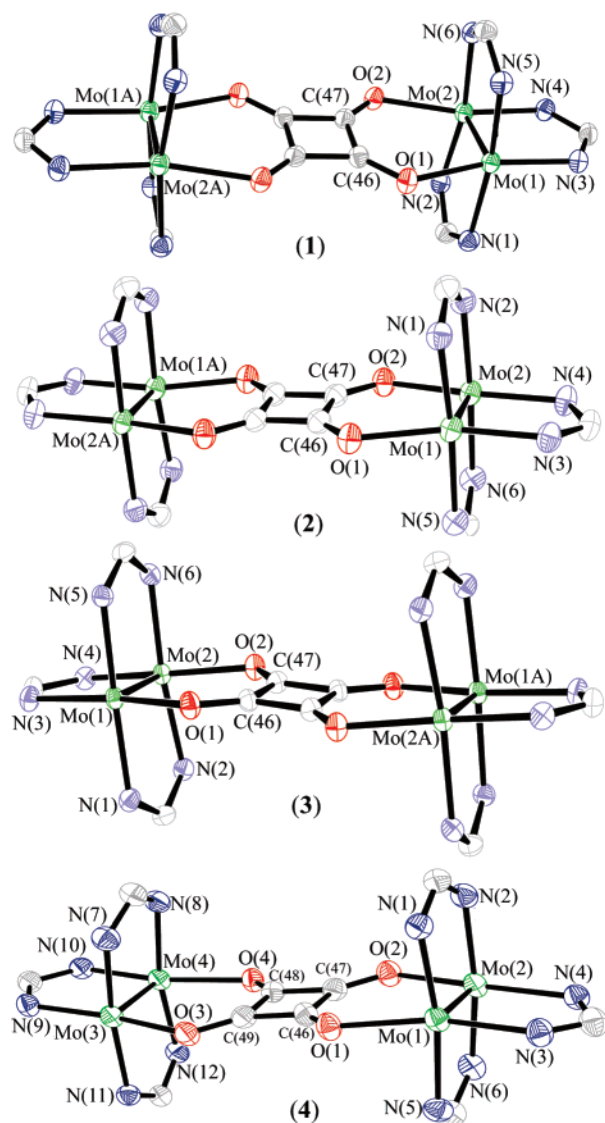


**Figure 1.** Core structures for compounds **1**–**4**. Thermal ellipsoids are drawn at the 50% probability level. All *p*-anisyl and *m*-trifluoromethylphenyl groups, hydrogen atoms, and the anions in **3** and **4** have been omitted for clarity.

through two C–C bonds. The two parallel Mo–Mo bonds, squarate ligand, and six-membered rings are all essentially coplanar.

Compounds **1** and **2** both crystallize in space group  $P\bar{1}$  with  $Z = 1$ , with each molecule residing on a crystallographic inversion center. The independent Mo–Mo bond distances of 2.1083(7) Å for **1** and 2.102(1) Å for **2** (Table 1) are in the normal range for quadruple Mo–Mo bonds with  $\sigma^2\pi^4\delta^2$  electronic configurations.<sup>24</sup> The midpoints of the Mo–Mo bonds are separated by 7.537 and 7.514 Å in **1** and **2**, respectively.

The squarate moieties in these compounds also have very similar structural features. For example, in **1** the independent C–C bond distances are nearly equal at 1.459(7) and 1.451(7) Å and similarly in **2** these are 1.452(6) and 1.464(7) Å.

These distances are significantly longer than those in phenyl rings (e.g., 1.38–1.40 Å in  $C(C_6H_5)_4$ )<sup>25</sup> but shorter than expected for singly bonds such as that of 1.553(3) Å for the  $C_{\text{central}}-C_{\text{phenyl}}$  in  $C(C_6H_5)_4$  or 1.55(2) Å for the C–C bonds in acetone<sup>26</sup> but are closer to the C–C distances in glyoxal and acetaldehyde (1.47(2) and 1.493 Å, respectively).<sup>26</sup> The C–C distances in the squarate units are consistent with only limited conjugation within the  $C_4$  unit but a small degree of delocalization of the  $\pi$ -electrons cannot entirely be ruled out. The short C–O bond distances (1.263(6) and 1.257(6) Å in **1** and 1.256(6) and 1.255(5) Å in **2**) are close to those commonly found in C=O double bonds (ca. 1.20 Å) but much shorter than typical C–O single bond distances (ca. 1.43 Å).<sup>27</sup> Another important feature is that the Mo–O distances, 2.196(3) and 2.191(3) Å for **1** and 2.176(3) and 2.175(3) Å for **2**, are significant longer than those in molecular pairs that exhibit strong electronic coupling, which are usually about 2.06–2.11 Å.<sup>13,10,11a</sup> On the basis of these bond distances, the two six-membered rings connected by a four-member squarate ring are better represented as in Scheme 5a. To a certain degree this unit resembles a heterobiphenylene where the  $d\pi$  and  $p\pi$  electrons are more or less localized in each hetero six-membered ring in order to minimize the antiaromatic character of four-electron  $\pi$ -bonding within the cyclobutadiene ring.

In contrast to **1** and **2**, the core of **3**, the singly oxidized product of **2**, has a nonplanar core. This compound also crystallizes in space group  $P\bar{1}$  with  $Z = 1$ ; thus, the cation also possesses a crystallographic inversion center. The crystallographically equivalent Mo–Mo distances (2.1247(8) Å) are about 0.025 Å longer than those in **2**. The elongation is similar to the change in distance when the di-*p*-anisloxamidate-bridged analogue loses one electron.<sup>11b</sup> These data are consistent with the removal of only one electron from a  $\delta$  MO of the neutral compound **2**. In this mixed-valence compound, the distance between the midpoints of the two Mo–Mo bonds decreases to 7.436 Å relative to that in its precursor (7.514 Å). This decrease can be attributed to the shortening in Mo–O bond distances as the oxidation state in Mo atoms increases. Upon oxidation, the bond distances O–C and C–C in the squarate linker remain unchanged within detection limits.

Compound **4**, the doubly oxidized product of **1**, is composed of a  $\{[Mo_2(DAniF)_3]_2(\mu_4-C_4O_4)\}^{2+}$  dication and two TFPB monoanions. It also crystallizes in the triclinic space group  $P\bar{1}$  but with the molecule residing on a general position. The  $C_4O_4^{2-}$  dianion is essentially planar, but one  $Mo_2$  unit is about 0.1 Å below the plane and the other one about 0.35 Å above the plane.

The Mo–Mo bonds are parallel to each other, and the distance between their midpoints of 7.442 Å is about 0.10 Å shorter than that of 7.537 Å in **1**. This decrease is mainly

(24) (a) Lawton, D.; Mason, R. *J. Am. Chem. Soc.* **1965**, *87*, 921. (b) Cotton, F. A.; Mester, Z. C.; Webb, T. R. *Acta Crystallogr.* **1974**, *B30*, 2768. (c) Cotton, F. A.; Daniels, L. M.; Hillard, E. A.; Murillo, C. A. *Inorg. Chem.* **2002**, *41*, 1639.

(25) Robbins, A.; Jeffrey, G. A.; Chesik, J. P.; Donohue, J.; Cotton, F. A.; Frenz, B. A.; Murillo, C. A. *Acta Crystallogr.* **1975**, *B31*, 2395.

(26) (a) Glockler, G. *J. Phys. Chem.* **1958**, *62*, 1049. (b) Smith, M. B.; March, J. *Advanced Organic Chemistry*, 5th ed. Wiley: New York, 2001; p 20.

(27) Cottrell, T. L. *The Strengths of Chemical Bonds*, 2nd ed.; Butterworth: London, 1958.

**Table 1.** Selected Distances (Å) and Angles (deg) for **1–4**

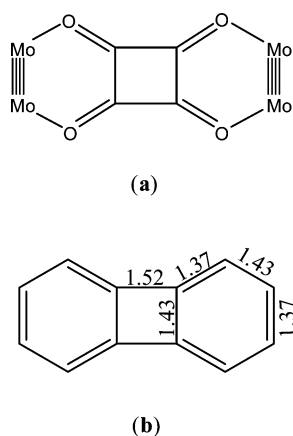
	<b>1</b> ·3CH <sub>2</sub> Cl <sub>2</sub>	<b>2</b> ·1.5C <sub>2</sub> H <sub>5</sub> OH·0.5CH <sub>2</sub> Cl <sub>2</sub>	<b>3</b> ·3CH <sub>2</sub> Cl <sub>2</sub>	<b>4</b> ·3.5CH <sub>2</sub> Cl <sub>2</sub> ·0.5C <sub>6</sub> H <sub>14</sub> <sup>a</sup>
Mo(1)–Mo(2)	2.1083(7)	2.102(1)	2.1247(8)	2.1504(7)
Mo <sub>2</sub> ···Mo <sub>2</sub> <sup>b</sup>	7.537	7.514	7.436	7.442
Mo(1)–O(1)	2.196(3)	2.176(3)	2.142(4)	2.128(3)
Mo(2)–O(2)	2.191(3)	2.175(3)	2.137(4)	2.158(3)
O(1)–C(46)	1.263(6)	1.256(6)	1.265(7)	1.248(6)
O(2)–C(47)	1.257(6)	1.255(5)	1.254(7)	1.253(6)
C(46)–C(47)	1.459(7)	1.452(6)	1.455(8)	1.471(7)
C(46)–C(47A)	1.451(7)	1.464(7)	1.448(8)	
C(46)–C(49)				1.457(7)
C(47)···C(47A) <sup>c</sup>	2.069	2.064	2.063	
C(47)···C(49) <sup>c</sup>				2.070(7)
Mo(1)–N(1)	2.146(4)	2.135(4)	2.124(5)	2.134(4)
Mo(1)–N(3)	2.122(4)	2.105(4)	2.118(5)	2.054(4)
Mo(1)–N(5)	2.138(4)	2.154(4)	2.126(5)	2.115(4)
Mo(2)–N(2)	2.142(4)	2.136(4)	2.127(5)	2.106(4)
Mo(2)–N(4)	2.115(4)	2.119(4)	2.094(5)	2.090(4)
Mo(2)–N(6)	2.151(4)	2.144(4)	2.130(5)	2.106(4)
N(1)–Mo(1)–N(3)	93.80(15)	95.60(15)	93.01(18)	90.44(16)
N(3)–Mo(1)–N(5)	90.57(15)	87.63(15)	91.97(18)	97.18(16)
N(1)–Mo(1)–O(1)	86.17(14)	88.02(14)	86.23(17)	83.34(14)
N(5)–Mo(1)–O(1)	88.10(14)	87.53(13)	87.67(17)	88.22(14)
N(4)–Mo(2)–N(6)	92.54(15)	87.87(15)	92.01(18)	97.39(16)
N(2)–Mo(2)–N(4)	93.59(15)	96.22(15)	93.24(18)	92.26(16)
N(6)–Mo(2)–O(2)	85.38(13)	87.61(14)	90.38(17)	86.78(14)
N(2)–Mo(2)–O(2)	87.29(14)	86.93(14)	83.49(17)	82.79(15)

<sup>a</sup> **4** has idealized C<sub>2</sub> symmetry. <sup>b</sup> Distances between the midpoints of the [Mo<sub>2</sub>] units. <sup>c</sup> Nonbonded separations between diagonal carbon atoms in the squarate units.

**Table 2.** Electrochemical Data for **1**, **2**, and Selected [Mo<sub>2</sub>(DAniF)<sub>3</sub>](L)[Mo<sub>2</sub>(DAniF)<sub>3</sub>] Compounds<sup>a</sup>

L	Mo <sub>2</sub> ···Mo <sub>2</sub> (Å)	E <sub>1/2</sub> (+1/0) <sup>b</sup> (mV)	E <sub>1/2</sub> (+2/+1) <sup>b</sup> (mV)	ΔE <sub>1/2</sub> (mV)	K <sub>C</sub> <sup>c</sup>	ref
<b>1</b>	7.537	79	357	278	5.01 × 10 <sup>4</sup>	this work
<b>2</b>	7.514	518	675	157	4.51 × 10 <sup>2</sup>	this work
<sup>-</sup> O <sub>2</sub> CCO <sub>2</sub> <sup>-</sup>	6.953	260	472	223 <sup>d</sup>	5.9 × 10 <sup>3</sup>	8a
<sup>-</sup> O <sub>2</sub> CCH <sub>2</sub> CO <sub>2</sub> <sup>-</sup>	7.647	225	285	108 <sup>d</sup>	67	8a
α-diphenyloxamidate	7.096	176	367	191	1.7 × 10 <sup>3</sup>	11a
β-diphenyloxamidate	6.322	-157	383	540	1.3 × 10 <sup>9</sup>	11a
β-dimethyloxamidate	6.248	-169	362	531	9.5 × 10 <sup>8</sup>	10
C <sub>6</sub> H <sub>2</sub> O <sub>4</sub> <sup>2-</sup> (dhbq <sup>2-</sup> )	8.536	-200	563	763	7.92 × 10 <sup>12</sup>	13
cis-1,5-dihydroxy-2,4-di(methylamino)benzene	8.816	310	1160	850	2.34 × 10 <sup>14</sup>	14

<sup>a</sup> All potentials are referenced to Ag/AgCl. <sup>b</sup> E<sub>1/2</sub> = (E<sub>pa</sub> + E<sub>pc</sub>)/2 from the CV for compounds **1** and **2**. <sup>c</sup> K<sub>C</sub> is calculated using the formula K<sub>C</sub> = exp(ΔE<sub>1/2</sub>/25.69). See ref 29b. <sup>d</sup> Calculated using the DPV peak half-height method of Richardson and Taube, see ref 29b.

**Scheme 5**

due to the shrinkage of the Mo–O bonding distances (by about 0.04 Å) upon oxidation. The Mo–Mo bond distances of 2.1504(7) and 2.1541(7) Å are essentially the same as that in Mo<sub>2</sub>(DAniF)<sub>4</sub><sup>+</sup>.<sup>5d</sup> These distances are longer by ca. 0.04 Å from 2.1083(7) Å in **1** and are about 0.026 Å longer than those in the singly oxidized compound **3**. This is consistent with the presence of two identical Mo<sub>2</sub><sup>5+</sup> moieties.

The Mo–O bond distances decrease even more as the second electron is removed. However, the average C–C and C–O distances in the squarate linker are essentially the same as those in the precursor **1** and the singly oxidized species **3**.

**Electrochemistry.** Electrochemical data are commonly and conveniently used to classify the mixed-valence compounds according to the Robin and Day classification,<sup>28</sup> and provide useful information about the degree of the interaction between redox centers.<sup>29,30</sup> Electrochemical data for the neutral compounds **1** and **2** are summarized in Table 2 and Figure 2. The cyclic voltammograms (CVs) and differential pulse voltammograms (DPVs) show two well-separated reversible waves. The two redox processes are [Mo<sub>2</sub>]-centered (vide infra), and they correspond to the oxidation of each neutral compound to a singly ([Mo<sub>2</sub>]L[Mo<sub>2</sub>]<sup>+</sup>) and a doubly oxidized species ([Mo<sub>2</sub>]L[Mo<sub>2</sub>]<sup>2+</sup>).

(28) Robin, M. B.; Day, P. *Adv. Inorg. Chem. Radiochem.* **1967**, *10*, 357.

(29) (a) Cannon, R. D. *Electron-Transfer Reactions*, Butterworth: London, 1980. (b) Richardson, D. E.; Taube, H. *Inorg. Chem.* **1981**, *20*, 1278.

(30) It should be noted that caution should be used especially when non-innocent linkers are present in the compounds under study. This is why interpretation should always be accompanied by analysis of additional data such as those from structural, spectroscopic, or magnetic studies.

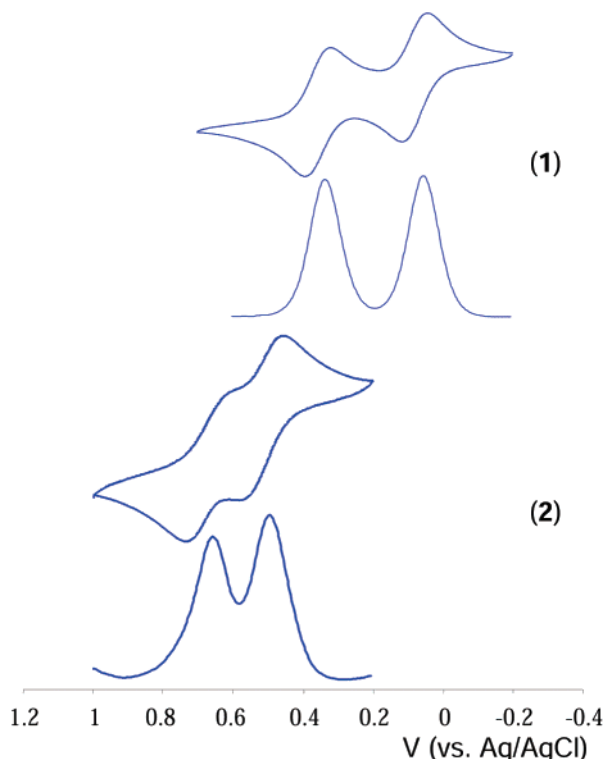


**Figure 2.** CVs and DPVs for compounds **1** (upper) and **2** (lower). These electrochemical measurements were recorded in  $\text{CH}_2\text{Cl}_2$  solution. The potentials, in V, are referenced to Ag/AgCl.

The redox potentials,  $E_{1/2}$ , for **1** in  $\text{CH}_2\text{Cl}_2$  are at 79 and 357 mV, which gives  $\Delta E_{1/2}$  value of 278 mV. From this value, the comproportionation constant,  $K_C$ , can be calculated using the relationship  $K_C = \exp(\Delta E_{1/2}/25.69)$ .<sup>31</sup> This gives a low value of  $5.01 \times 10^4$ , which indicates that the two  $[\text{Mo}_2]$  centers in **1** are only loosely coupled by the squarate ligand and the singly oxidized species is not thermodynamically favored. Because the distance of 7.516 Å between  $[\text{Mo}_2]$  units in this compound is close to that of 7.647 Å in the analogous molecular pair  $[\text{Mo}_2](\text{O}_2\text{CCH}_2\text{CO}_2)[\text{Mo}_2]$ ,<sup>8a</sup> it is of interest to compare their electrochemical behavior. It should be noted since there is no delocalized  $\pi$  orbital in the  $\text{O}_2\text{CCH}_2\text{CO}_2$  linker, the electronic coupling in  $[\text{Mo}_2](\text{O}_2\text{CCH}_2\text{CO}_2)[\text{Mo}_2]$  which has  $\Delta E_{1/2}$  of 108 mV is mainly attributed to electrostatic interactions. To a first approximation, the difference between the  $\Delta E_{1/2}$  values for these two compounds suggests that the contribution from the mediation of the squarate ligand in the electronic coupling is about 170 mV. Comparison with the oxalate analogue which has a  $\Delta E_{1/2}$  of 223 mV and a distance of 6.953 Å between  $[\text{Mo}_2]$  units shows that the squarate group is a slightly better electronic communicator than the oxalate anions.

A more important comparison can be made with the analogue that has a  $\text{C}_6$  ring instead of a  $\text{C}_4$  ring. In the compound with the anion of 2,5-dihydroxy-1,4-benzoquinone ( $\text{d}h\text{b}q^{2-}$ ) as linker (**III**),<sup>13</sup> the  $K_C$  is about 8 orders of magnitude larger ( $7.92 \times 10^{12}$ ). Structural data suggest that

the strong electron delocalization extends through the periphery of the 14-atom ring that includes the linker and the four Mo atoms, as shown to a first approximation in Scheme 1. Great differences in bond distances in the heterocyclic cores between the  $\text{d}h\text{b}q^{2-}$ -bridged complex (**I**, where  $X = \text{H}$ ) and squarate bridged compounds (**1** and **2**) are shown in Table 3. The complex, illustrated in **I** and Table 3, shows large variations in C–C (*A* and *B*) distances, while in **1** and **2**, the *A* and *B* distances, ca. 1.46 Å, are similar, and both deviate little from C–C single bonds and the *B* distances in **I**. The average C–O (*C*) distances, 1.260[8] Å in **1** and 1.256[8] Å in **2**, are longer than those of the resonant C–O bonds in **I** (1.296[4] Å) but close to typical C=O double bond distances (1.20 Å). Additionally, the very long Mo–O (*D*) distances (2.194[4] Å in **1** and 2.176[4] Å in **2**) are much longer than those in **I**, suggesting that the  $\delta$  electrons are localized in each  $\text{Mo}_2$  unit and the  $p\pi$  electrons in the squarate linker are not delocalized within the ring but contribute to the formation of C=O double bonds, as shown in a simplified manner in Scheme 5a. The unit composed of the  $\text{Mo}_2$  bonds and the squarate ligand resembles a hetero-biphenylene where the  $d\pi$  and  $p\pi$  electrons are localized and alternative single and double bonds form between the carbon atoms, similarly to what is observed in biphenylene as shown in Scheme 5b (bond distances in Å).<sup>32</sup> This structural analysis show a great difference between the  $\text{d}h\text{b}q^{2-}$ -bridged complex (**I**) and squarate bridged compounds (**1** and **2**) that is consistent with the electrochemistry results.

It should be noted that even though **1** and **2** have a  $\text{C}_4\text{O}_4^{2-}$  bridging group, their peripheral formamidate ligands are different and this also influences their electrochemical behavior. The CV for **2** in  $\text{CH}_2\text{Cl}_2$  has two consecutive one-electron redox processes at 518 and 675 mV. The redox potentials show positive shifts of 439 and 318 mV compared to those for **1**. This shift is consistent with the presence of the electron-withdrawing substituents on the formamidate in **2** but electron-donating groups in **1**. The  $\Delta E_{1/2}$  value of 157 mV for **2** is 121 mV smaller than that for **1**, demonstrating that the electronic properties of peripheral ligands also have a significant influence on the electronic communication between redox centers.

The electrochemical data suggest that the unpaired electron in **3** is localized on one of the  $\text{Mo}_2$  units. This description is also consistent with the lack of charge-transfer bands in the NIR spectra taken in the region from 2000 to 12000  $\text{cm}^{-1}$  both in the solid state and in acetone. This is consistent with the singly oxidized species **3** being electronically localized in the time scale of the NIR measurement ( $10^{-14}$  s).<sup>33</sup> Because the crystal structure of **3** show that the two  $\text{Mo}_2$  bonds are equivalent, it is plausible that there is a disordered distribution of the two  $[\text{Mo}_2]$  units in the crystal.<sup>34</sup>

(31) See for example: (a) Flanagan, J. B.; Margel, S.; Bard, A. J.; Anson, F. C. *J. Am. Chem. Soc.* **1978**, *100*, 4248. (b) Ito, T.; Hamaguchi, T.; Nagino, H.; Yamaguchi, T.; Kido, H.; Zavarine, I. S.; Richmond, T.; Washington, J.; Kubiak, C. P. *J. Am. Chem. Soc.* **1999**, *121*, 4625.

(32) Andres, W.; Günther, H.; Günther, M.-E.; Hausmann, H.; Jikeli, G.; Puttkamer, H.; Schmicker, H.; Niu-Schwarz, J.; Schwarz, W. H. E. *Helv. Chim. Acta* **2001**, *84*, 1737.

(33) Lever, A. B. P. In *Comprehensive Coordination Chemistry II*, McCleverty, J. A., Meyer, T. J., Eds.; Elsevier Science: Oxford, 2004; Vol. 2, pp 435–438.

(34) This again shows the importance of using data from various experimental techniques to ascertain whether a species is electronically localized or delocalized. See ref 30.



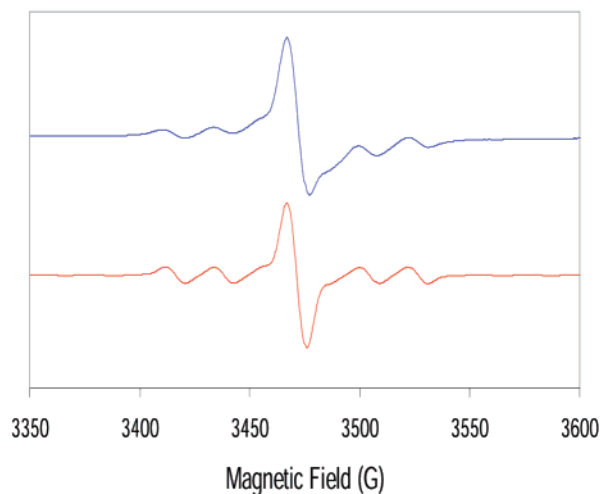


**Figure 3.** EPR spectrum of **4** in  $\text{CH}_2\text{Cl}_2$  at ambient temperatures (blue). The red trace below is the simulated spectrum.

**EPR Properties and Magnetic Measurements.** X-band EPR spectroscopy has also been employed for the study of complexes **3** and **4**, which have formally one or two  $\text{Mo}_2^{5+}$  units. For the singly oxidized species **3**, the EPR spectrum was measured at ambient temperature in the solid state. Only one prominent signal was observed, which is consistent with a doublet electronic ground state. The  $g$  value of 1.949 is significantly different from that for an organic free radical, indicating that the unpaired electron in **3** resides in a mainly metal-based orbital. The main peak is due to molecules containing only the  $^{96}\text{Mo}$  ( $I = 0$ ) isotope (about 74% abundance).

The spectrum for the doubly oxidized species **4** measured in  $\text{CH}_2\text{Cl}_2$  solution at room temperature exhibits a prominent peak ( $g = 1.953$ ) and several hyperfine lines (Figure 3). The simulated spectrum shows satisfactory agreement with the experimental results and gives a hyperfine coupling constant  $A = 20.1 \times 10^{-4} \text{ cm}^{-1}$ ,<sup>35</sup> which is comparable to the value of  $22 \times 10^{-4} \text{ cm}^{-1}$  obtained from  $\{\text{Mo}_2(\text{DAniF})_4\}^+$  in which the unpaired electron is coupled to only two Mo atoms.<sup>5d</sup> This indicates that the two unpaired electrons in the doubly oxidized species **4** are localized on one dimetal unit in the time scale ( $1.68 \times 10^{-11} \text{ s}$ ) of the EPR measurement at 9.5 GHz.<sup>36</sup> It should be noted that in a Robin–Day class III species, the two unpaired electrons would be expected to be coupled and the dication would be diamagnetic.

Because there is one unpaired electron at each of the two  $[\text{Mo}_2]$  units in **4**, it is also useful to study the electronic coupling between the two spatially separated odd electrons

(35) For comparison the hyperfine coupling constant  $A$  values for the weakly coupled compounds are  $22 \times 10^{-4} \text{ cm}^{-1}$  for  $\{[\text{Mo}_2](N,N'-diethylterephthalamidate) $[\text{Mo}_2]\}^+$  and  $27.2 \text{ G}$  ( $27.2 \times 10^{-4} \text{ cm}^{-1}$ ) for  $\{[\text{Mo}_2](\text{perfluoroterephthalate})[\text{Mo}_2]\}^+$ . See: (a) Cotton, F. A.; Li, Z.; Liu, C. Y.; Murillo, C. A. *Inorg. Chem.* **2006**, *45*, 9765. (b) Chisholm, M. H.; Pate, B. D.; Wilson, P. J.; Zaleski, J. M. *Chem. Commun.* **2002**, 1084.$

(36) The timescale is given by  $(2\pi\nu)^{-1}$ , where the  $\nu$  is the operating frequency. See: (a) Weil, J. A.; Bolton, J. R.; Wertz, J. E. *Electron Paramagnetic Resonance Spectroscopy: Elementary Theory and Practical Applications*; Wiley: New York, 1994. (b) Dei, A.; Gatteschi, D.; Sangregorio, C.; Sorace, L.; Vaz, M. G. F. *Chem. Phys. Lett.* **2003**, *368*, 162.

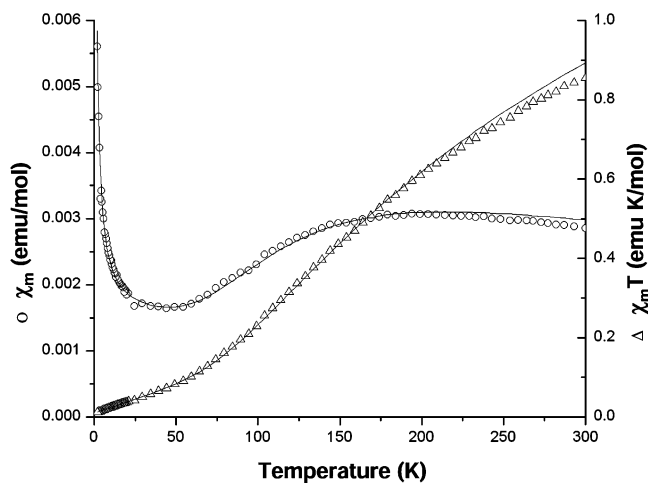


**Figure 4.** Plots of  $\chi_m T$  ( $\Delta$ ) and  $\chi_m$  ( $\circ$ ) vs  $T$  for **4**. The solid line is the theoretical fit using the parameters given in the text.

using magnetic measurements. Magnetic susceptibilities plotted versus temperature (Figure 4) clearly show a broad maximum around 100–200 K, which indicates the presence of antiferromagnetic coupling between the two odd electrons. The increase in susceptibilities with decreasing temperature in the very low temperature region is often seen in antiferromagnetically coupled systems.<sup>37</sup> The magnetic susceptibilities were fitted to eq 3 for antiferromagnetically coupled  $S = 1/2$  dimers<sup>38</sup> with allowance for a paramagnetic fraction,  $P$ , and temperature-independent paramagnetism (TIP), arising from possible impurities in the sample.

$$\chi = \frac{2Ng^2\beta^2}{kT} \left[ (1 - P) \left[ \frac{\exp(2J/kT)}{1 + 3 \exp(2J/kT)} \right] + \frac{P}{4} \right] + \text{TIP} \quad (3)$$

The best fit values of  $J$ ,  $P$ , and TIP were  $-121 \text{ cm}^{-1}$ , 0.0124, and  $0.00143 \text{ cm}^3 \text{ mol}^{-1}$ , respectively. The best fit was the one which minimized the function  $F$  in eq 4.

$$F = \left[ \frac{1}{n} \sum_{i=1}^n \left( \frac{\chi_{\text{calcd}}^i - \chi_{\text{obs}}^i}{\chi_{\text{obs}}^i} \right)^2 \right]^{1/2} \quad (4)$$

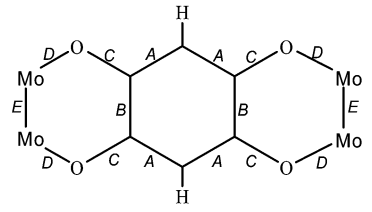
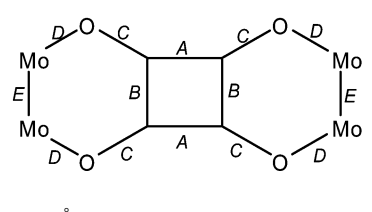
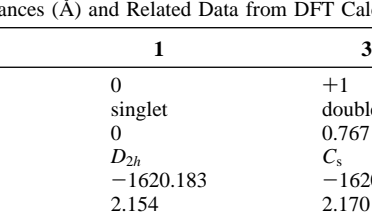
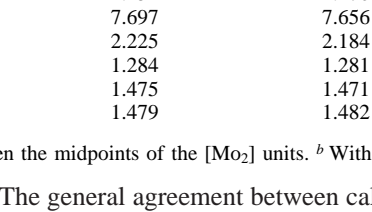
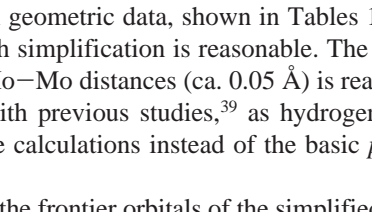
The value of  $F$ , which provided a measure of agreement between experimental data and the simulation, was 0.0253. The magnetic measurements indicate that the two odd electrons in  $[\text{Mo}_2]$  units of doubly oxidized species **4** are only weakly antiferromagnetically coupled, which is consistent with the electrochemical data.

**Electronic Structures and DFT Calculations.** The DFT calculations were done using the model  $[\text{Mo}_2(\text{NHCHNH})_3]_2(\mu\text{-C}_4\text{O}_4)$  and parameters from the crystal structure as a starting point. The models for the neutral compounds were optimized by imposing  $D_{2h}$  symmetry constraints, while those for the oxidized species had the lower symmetry  $C_s$  to ensure

(37) (a) Burojevic, S.; Shroeky, I.; Bino, A.; Summers, D. A.; Thompson, R. C. *Inorg. Chim. Acta* **1996**, *251*, 75. (b) Sun, Y.; Melchior, M.; Summers, D. A.; Thompson, R. C.; Rettig, S. J.; Orvig, C. *Inorg. Chem.* **1998**, *37*, 3119.

(38) Bleaney, B.; Bowers, K. D. *Proc. R. Soc. London, Ser. A* **1952**, *214*, 451.

**Table 3.** Comparison in Selected Average Bond Distance (Å) between the Benzoquinone Derivative (**1**,  $\text{d}h\text{bq}^{2-}$ , Ref 13) and Squarate Linked Complexes

	<b>1</b>	<b>1</b>	<b>2</b>
	1.389[4]	1.451(7)	1.464(7)
	1.481(4)	1.459(7)	1.452(6)
	1.296[4]	1.260[8]	1.256[8]
	2.060[3]	2.194[4]	2.176[4]
	2.1051(4)	2.1083(7)	2.102(1)

**Table 4.** Bond Distances (Å) and Related Data from DFT Calculations for Models of **1**, **3**, and **4**

compounds	<b>1</b>	<b>3<sup>b</sup></b>	<b>4<sup>b</sup></b>
charge	0	+1	+2
spin	singlet	doublet	singlet
$S^2$	0	0.767	0
symmetry	$D_{2h}$	$C_s$	$C_s$
energy (au)	-1620.183	-1620.011	-1619.711
Mo(1)-Mo(2)	2.154	2.170	2.188
Mo <sub>2</sub> ...Mo <sub>2</sub> <sup>a</sup>	7.697	7.656	7.639
Mo(1)-O(1)	2.225	2.184	2.150
O(1)-C(46)	1.284	1.281	1.278
C(46)-C(47)	1.475	1.471	1.470
C(46)-C(47A)	1.479	1.482	1.488

<sup>a</sup> Distances between the midpoints of the [Mo<sub>2</sub>] units. <sup>b</sup> With idealized  $D_{2h}$  symmetry.

higher accuracy. The general agreement between calculated and experimental geometric data, shown in Tables 1 and 4, suggests that such simplification is reasonable. The overestimation of the Mo-Mo distances (ca. 0.05 Å) is reasonable and consistent with previous studies,<sup>39</sup> as hydrogen atoms were used for the calculations instead of the basic *p*-anisyl groups.

An analysis of the frontier orbitals of the simplified model indicates that even though the squarate linker has some involvement in the electronic coupling between the two dimetal units, the percentage of linker character is very small, as seen in the orbital diagram (Figure 5). For this model the HOMO has 61.28% metal character and only 17.58% linker character. The remaining 21.14% corresponds to the contribution from the supporting formamidinate ligands. The linker-based orbitals are the unoccupied LUMO which has an energy of 2.62 eV above HOMO, and the HOMO-2 that has an energy of 1.86 eV below the HOMO. Because the energy differences between the LUMO or HOMO-2 and the HOMO are quite large, neither the LUMO or HOMO-2 contribute much to the electronic coupling involving the two  $\delta$  orbitals, as these large energy gaps prevent electron-hopping or hole-hopping pathways that generally facilitate electron transfer.<sup>40</sup>

The orbital interaction diagram (Figure 6) shows that the overlap between metal-based  $\delta$  orbitals and the HOMO from

the squarate linker (shown in red), and between  $\delta$  orbitals and LUMO from the linker (shown in blue) is indeed very poor. Thus, the HOMO is a mainly metal-based orbital with a very small linker contribution and the HOMO-2 is a mainly linker-based orbital. The small linker character in the HOMO and the reduced overlap between the metal orbitals and linker orbitals are in agreement with the weak electronic coupling observed by electrochemistry. This is also consistent with the observed weaker electronic interaction in **2** than in **1** because the electron-withdrawing groups on the formamidate in **2** are expected to decrease the energy of the  $\delta$  orbitals. This increases the energy difference between metal-based  $\delta$  orbitals and the linker-based LUMO orbital (shown in blue in Figure 6), which results in lesser orbital overlap and weaker electronic communication.

It should be noted that compounds **1** and **2** resemble biphenylene not only in the atom arrangement but also in electronic structure.<sup>41</sup> A comparison of the frontier molecular orbitals of biphenylene and those of **1** is shown in Figure 7. The isolobality of the LUMO and HOMO-2 from **1** and the biphenylene LUMO and HOMO-3, respectively, is noticeable.

For the doubly oxidized species **4**, the magnetic exchange coupling constant  $J$  between the two unpaired electrons was theoretically evaluated using models for three different spin states. The first was a singlet ( $S = 0$ ) model that assumes the antiferromagnetically coupled restricted singlet state which would be expected for a species with large electronic

(39) Cotton, F. A.; Donahue, J. P.; Murillo, C. A.; Pérez, L. M. *J. Am. Chem. Soc.* **2003**, *125*, 5486.

(40) Chisholm, M. H.; Clark, R. J. H.; Gallucci, J.; Hadad, C. M.; Patmore, N. *J. Am. Chem. Soc.* **2004**, *126*, 8303.

(41) Vogler, H.; Ege, G. *J. Am. Chem. Soc.* **1977**, *99*, 4599.



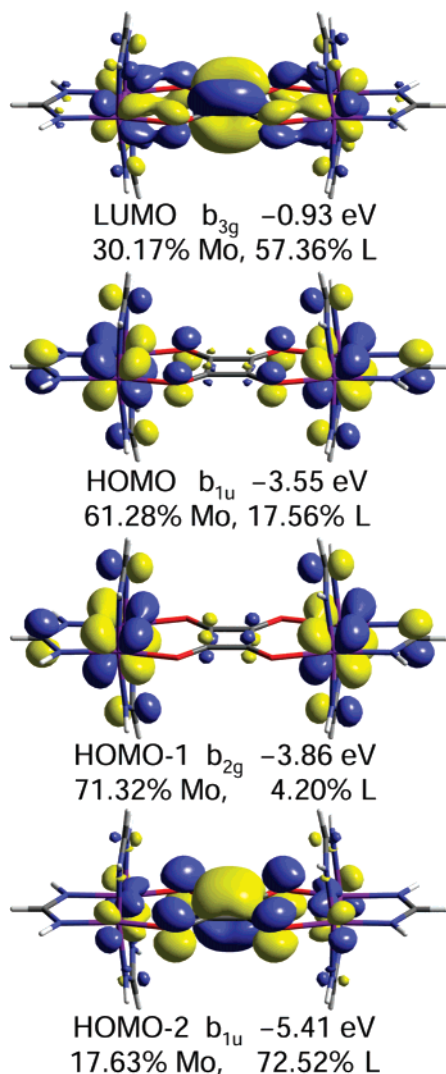


**Figure 5.** Selected frontier orbital plots calculated for the simplified model of **1** in which the *p*-anisyl groups were replaced by hydrogen atoms. Orbitals are drawn using an isosurface value of 0.03. The percentage values are for molybdenum and linker (L) character. The difference from 100% corresponds to the contribution of the formamidate ligands.

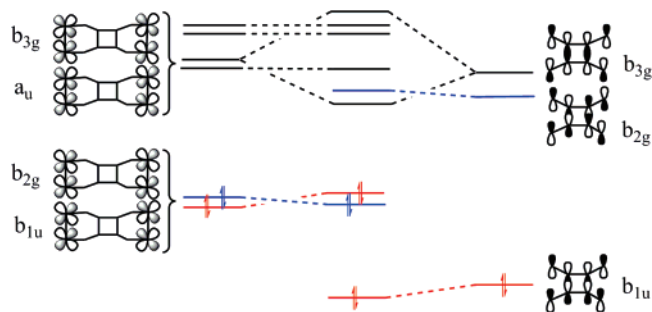


**Figure 6.** Orbital interaction diagram for **1**. The column on the left shows the frontier orbitals from the dimetal units, and the right column has the linker orbitals.

communication; the second was a triplet state ( $S = 1$ ) that describes a ferromagnetic interaction between the two unpaired electrons; the third was a broken-symmetry (BS) model at an antiferromagnetically coupled unrestricted singlet state. The latter gave the lowest energy among the three models and yielded  $J^{\text{GND}} = -130 \text{ cm}^{-1}$ , calculated by the

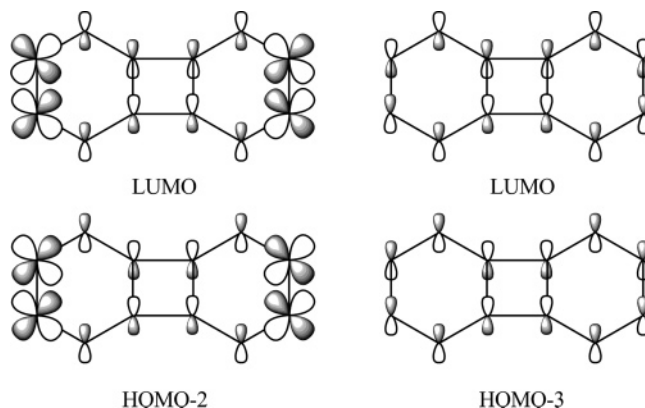


**Figure 7.** Comparison of the frontier orbitals for **1** (left) and biphenylene (right).

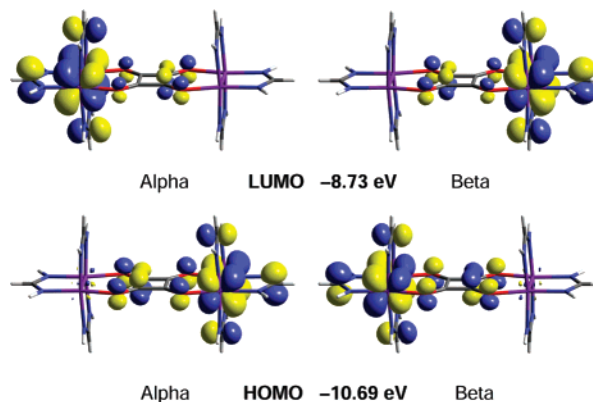


**Figure 8.** LUMO (upper) and HOMO (lower) orbitals from broken-symmetry calculations of the  $\{[\text{Mo}_2(\text{HCNHCH})_3]_2(\text{C}_4\text{O}_4)\}^{2+}$  model. Orbitals are drawn using an isosurface value of 0.03.

so-called Ginsberg,<sup>42</sup> Noodleman,<sup>43</sup> and Davidson<sup>44</sup> (GND) spin projected equation (eq 5).<sup>45</sup> These DFT calculations closely reproduce the experimental  $J$  value of  $-121 \text{ cm}^{-1}$ .

$$J^{\text{GND}} = \frac{(\text{DFT}E_{\text{BS}} - \text{DFT}E_{\text{T}})}{S_{\text{max}}^2} \quad (5)$$

The BS state is actually an equal mixture of singlet and triplet states.<sup>46</sup> The electronic structure from the BS calculations shows that each of the unpaired electrons from the HOMO,  $\alpha$  and  $\beta$ , are localized on different dimolybdenum units, as shown in Figure 8. The ligand character for the HOMO in the antiferromagnetically coupled model is very small, which does not allow strong coupling between the

(42) Ginsberg, A. P. *J. Am. Chem. Soc.* **1980**, *102*, 111.

(43) (a) Noodleman, L. *J. Chem. Phys.* **1981**, *74*, 5737. (b) Noodleman, L.; Baerends, E. *J. Am. Chem. Soc.* **1984**, *106*, 2316. (c) Noodleman, L.; Peng, C. Y.; Case, D. A.; Mouesca, J.-M. *Coord. Chem. Rev.* **1995**, *144*, 199.

(44) Noodleman, L.; Davidson, E. R. *Chem. Phys.* **1986**, *109*, 131.

(45) A similar expression,  $J^{\text{Y}} = (\text{DFT}E_{\text{BS}} - \text{DFT}E_{\text{T}})/(\langle S^2 \rangle_{\text{T}} - \langle S^2 \rangle_{\text{BS}})$ , has also been reported by Yamaguchi et al., where  $E_{\text{T}}$  is the triplet energy in the unrestricted formalism using the BS orbitals. The BS calculations give a  $J^{\text{Y}}$  value of  $-252 \text{ cm}^{-1}$ , quite different from the  $J^{\text{GND}}$  which are usually used in the systems with relatively large orbital overlap. See: (a) Yamaguchi, K.; Takahara, Y.; Fueno, T.; Nasu, K. *Jpn. J. Appl. Phys.* **1987**, *26*, L1362. (b) Yamaguchi, K.; Jensen, F.; Dorigo, A.; Houk, K. N. *Chem. Phys. Lett.* **1988**, *149*, 537. (c) Soda, T.; Kitagawa, Y.; Onishi, T.; Takano, Y.; Shigeta, Y.; Nagao, H.; Yoshioka, Y.; Yamaguchi, K. *Chem. Phys. Lett.* **2000**, *319*, 223.

(46) Ciofini, I.; Dual, C. A. *Coord. Chem. Rev.* **2003**, *238–239*, 187.

**Table 5.** X-ray Crystallographic Data

compound	1·3CH <sub>2</sub> Cl <sub>2</sub>	2·1.5C <sub>2</sub> H <sub>5</sub> OH·0.5CH <sub>2</sub> Cl <sub>2</sub>	3·3CH <sub>2</sub> Cl <sub>2</sub>	4·3.5CH <sub>2</sub> Cl <sub>2</sub> ·0.5C <sub>6</sub> H <sub>14</sub>
chemical formula	C <sub>97</sub> H <sub>96</sub> Cl <sub>6</sub> Mo <sub>4</sub> N <sub>12</sub> O <sub>16</sub>	C <sub>97.5</sub> H <sub>64</sub> ClF <sub>36</sub> Mo <sub>4</sub> N <sub>12</sub> O <sub>5.5</sub>	C <sub>97</sub> H <sub>60</sub> Cl <sub>6</sub> F <sub>42</sub> Mo <sub>4</sub> N <sub>12</sub> O <sub>4</sub> Sb	C <sub>164.5</sub> H <sub>128</sub> B <sub>2</sub> Cl <sub>7</sub> F <sub>48</sub> Mo <sub>4</sub> N <sub>12</sub> O <sub>16</sub>
fw	2282.32	2594.82	2973.78	4094.32
space group	P1(No. 2)	P1̄(No. 2)	P1̄(No. 2)	P1̄(No. 2)
a (Å)	10.270(3)	11.215(5)	10.635(3)	19.639(5)
b (Å)	16.383(4)	14.914(6)	14.747(4)	20.531(5)
c (Å)	16.750(4)	17.306(7)	19.804(5)	25.398(6)
α (deg)	67.296(4)	97.915(7)	103.889(4)	72.175(4)
β (deg)	88.776(5)	106.328(8)	104.596(4)	75.608(4)
γ (deg)	72.480(4)	104.691(6)	103.716(4)	67.363(4)
V (Å <sup>3</sup> )	2465(1)	2618(2)	2768(1)	8898(3)
Z	1	1	1	2
d <sub>calcd</sub> (g cm <sup>-3</sup> )	1.538	1.646	1.784	1.528
μ (mm <sup>-1</sup> )	0.730	0.615	0.953	0.494
T (K)	213(2)	213 (2)	213 (2)	183(2)
R1, <sup>a</sup> wR2 <sup>b</sup>	0.069, 0.135	0.068, 0.140	0.070, 0.138	0.094, 0.180
R1, <sup>a</sup> wR2 <sup>b</sup> (I > 2σ)	0.046, 0.120	0.050, 0.123	0.055, 0.128	0.057, 0.148

$$^a R1 = [\sum w(F_o - F_c)^2 / \sum wF_o^2]^{1/2}. \quad ^b wR2 = [\sum [w(F_o^2 - F_c^2)^2] / \sum w(F_o^2)^2]^{1/2}, \quad w = 1/[2(F_o^2) + (aP)^2 + bP], \quad \text{where } P = [\max(F_o^2, 0) + 2(F_c^2)]/3.$$

two dimetal units.<sup>47</sup> This is consistent with the weak antiferromagnetic coupling observed experimentally in the doubly oxidized compound **4**.

## Conclusions

Two neutral squarate linked *dimers of dimers* having quadruply bonded dimolybdenum units, **1** and **2**, were synthesized and fully characterized. The electrochemistry of the two neutral species indicates that there are only very weak electronic interactions between the two dimolybdenum units because the  $\pi$  electrons appear to be localized within the carbonyl and dimetal unit in the six-membered Mo<sub>2</sub>O<sub>2</sub>C<sub>2</sub> rings, an arrangement that minimizes the antiaromaticity in the central C<sub>4</sub> ring. The corresponding oxidized species are electronically localized in the time scale of the physical measurements. For the doubly oxidized complex **4** DFT calculations give a  $J$  value of  $-130 \text{ cm}^{-1}$ , very similar to that obtained from magnetic studies ( $J = -121 \text{ cm}^{-1}$ ), indicating that the two odd electrons are only weakly antiferromagnetically coupled. The DFT calculations also suggest that the energy mismatch of the frontier orbitals of the linker and dimetal units contributes to the low of communication between the Mo<sub>2</sub> units.

Compounds **1** and **2** structurally resemble benzoquinone (d**hbq**)<sup>13</sup> and N-substituted benzoquinonemonoimine analogues.<sup>14</sup> The main structural difference in the linkers is the presence of a central C<sub>4</sub> ring in **1** and **2** while there is a C<sub>6</sub> ring in the d**hbq** compound. This relatively small structural difference leads to dramatic changes in electronic communication ( $K_C$  differences of the order of 10<sup>8</sup>) between the dimolybdenum units. This shows the importance of the use of electrons in  $\delta$  orbitals in delocalizing electron density, a mechanism that is unavailable for analogues with single metal units. It is remarkable that structures that look so similar, squarate and the anion of dihydroxybenzoquinone, have comproportionation constants that differ by ca. 10<sup>8</sup>. These results show how electron conjugation that involves  $\delta$  bonds may be used to modulate electronic communication.

## Experimental Section

**Materials and Methods.** All procedures were performed under N<sub>2</sub> using either a N<sub>2</sub> dry box or standard Schlenk techniques. Solvents were distilled and/or degassed immediately prior to use. Dichloromethane, Et<sub>2</sub>O, and hexanes were purified under argon using a Glass Contour system; acetonitrile was twice distilled under N<sub>2</sub>, first from activated molecular sieves and then from CaH<sub>2</sub>. The salt (Bu<sub>4</sub>N)<sub>2</sub>C<sub>4</sub>O<sub>4</sub> was prepared as a white powder by reacting H<sub>2</sub>C<sub>4</sub>O<sub>4</sub> with 2 equiv of 1 M Bu<sub>4</sub>NOH in methanol followed by drying under vacuum overnight. The starting materials Mo<sub>2</sub>(DAniF)<sub>3</sub>-Cl<sub>2</sub><sup>48</sup> and [Mo<sub>2</sub>(DmCF<sub>3</sub>F<sub>3</sub>)<sub>2</sub>( $\mu$ -OH)<sub>2</sub>]<sup>22</sup> were prepared by literature methods. Other reagents were purchased from commercial sources and used as received.

**Physical and Characterization Measurements.** Elemental analyses were performed by Robertson Microлит Laboratories, Madison, NJ, on crystalline samples that were dried overnight under vacuum. The NMR spectra were recorded on an Inova NMR 300 spectrometer. The references used were the residual proton of CDCl<sub>3</sub> for the <sup>1</sup>H NMR spectra and CFC<sub>3</sub> in CDCl<sub>3</sub> for the <sup>19</sup>F NMR spectra. Absorption spectra in the range of 200–800 nm were measured at ambient temperature on a Shimadzu UV–2501 PC spectrophotometer. The NIR spectra were obtained from a Bruker TEASOR 27 spectrometer. EPR spectra were recorded using a Bruker ESP300 spectrometer, and the spectral simulations were done using the program WIN-EPR SimFonia provided by Bruker. Magnetic susceptibility measurements were performed on a SQUID magnetometer. The CVs and DPVs were taken with a CH Instruments Model-CH1620A electrochemical analyzer in 0.1 M Bu<sub>4</sub>NPF<sub>6</sub> solution in CH<sub>2</sub>Cl<sub>2</sub> with Pt working and auxiliary electrodes, a Ag/AgCl reference electrode, and a scan rate of 100 mV s<sup>-1</sup>. All potentials are referenced to the Ag/AgCl electrode, and under the present experimental conditions, the E<sub>1/2</sub> (Fc<sup>+</sup>/Fc) consistently occurred at +440 mV in CH<sub>2</sub>Cl<sub>2</sub>.

**Preparation of [Mo<sub>2</sub>(DAniF)<sub>3</sub>]<sub>2</sub>( $\mu$ -C<sub>4</sub>O<sub>4</sub>), **1**.** A mixture of Mo<sub>2</sub>(DAniF)<sub>3</sub>Cl<sub>2</sub><sup>48</sup> (670 mg, 0.650 mmol) and Zn powder (7.5 g) in 80 mL of CH<sub>3</sub>CN was stirred for 2 h, and the excess Zn then removed by filtration. The yellow filtrate was transferred to a Schlenk tube containing vacuum-dried (Bu<sub>4</sub>N)<sub>2</sub>C<sub>4</sub>O<sub>4</sub> (197 mg, 0.325 mmol), and the mixture was stirred at room temperature for 4 h. An orange precipitate was isolated by filtration, washed with 2 × 20 mL of diethyl ether, and dried under vacuum. Crystals used for

(47) Metal and linker character in  $\alpha$  and  $\beta$  HOMOs are 64.70% and 11.97%, respectively.

(48) Cotton, F. A.; Daniels, L. M.; Jordan, G. T., IV; Lin, C.; Murillo, C. A. *J. Am. Chem. Soc.* **1998**, *120*, 3398.

X-ray analysis were obtained by layering diethyl ether on top of a  $\text{CH}_2\text{Cl}_2$  solution. Yield: 350 mg (45%).  $^1\text{H}$  NMR (in  $\text{CDCl}_3$ , ppm): 8.841 (s, 4H, N-CH-N), 8.198 (s, 2H, N-CH-N), 6.554 (m, 32H, aromatic), 6.371 (d, 8H, aromatic), 6.123 (d, 8H, aromatic), 3.671 (s, 24H, - $\text{OCH}_3$ ), 3.622 (s, 12H, - $\text{OCH}_3$ ). UV-vis in  $\text{CH}_2\text{Cl}_2$ ,  $\lambda_{\text{max}}$  ( $\epsilon_{\text{M}}$ ,  $\text{M}^{-1} \text{cm}^{-1}$ ): 438 nm ( $9.41 \times 10^3$ ). Anal. Calcd for  $\text{C}_{94}\text{H}_{90}\text{N}_{12}\text{O}_{16}\text{Mo}_4$  (**1**): C, 55.45; H, 4.46; N, 8.26. Found: C, 55.34; H, 4.41; N, 8.15.

**Preparation of  $[\text{Mo}_2(\text{DmCF}_3\text{F})_3]_2(\mu_4\text{-C}_4\text{O}_4)$ , **2**.** To  $[\text{Mo}_2(\text{DmCF}_3\text{F})_3]_2(\mu\text{-OH})_2$  (480 mg, 2.00 mmol) and  $\text{H}_2\text{C}_4\text{O}_4$  (22.8 mg, 0.200 mmol) was added 30 mL of THF and 10 mL of methanol. This mixture was stirred at room temperature overnight. After removal of the solvent under reduced pressure, the residue was extracted with 10 mL of  $\text{CH}_2\text{Cl}_2$ . The filtrate was layered with 40 mL of ethanol. Red crystals of the product were obtained after the diffusion of ethanol was complete (about 1 week). Yield: 250 mg (50%).  $^1\text{H}$  NMR (in  $\text{CDCl}_3$ , ppm): 9.02 (s, 4H, N-CH-N), 8.30 (s, 2H, N-CH-N), 7.15–7.29 (m, 16H, aromatic), 6.87–7.06 (m, 24H, aromatic), 6.50 (d, 4H, aromatic), 6.00 (s, 4H, aromatic).  $^{19}\text{F}$  NMR (in  $\text{CDCl}_3$ , ppm): 109.88 (s, 24 F), 109.57 (s, 12 F). UV-vis in  $\text{CH}_2\text{Cl}_2$ ,  $\lambda_{\text{max}}$  ( $\epsilon_{\text{M}}$ ,  $\text{M}^{-1} \text{cm}^{-1}$ ): 407 nm ( $1.5 \times 10^4$ ). Anal. Calcd for  $\text{C}_{94}\text{H}_{54}\text{F}_{36}\text{Mo}_4\text{N}_{12}\text{O}_4$  (**2**): C, 45.47; H, 2.19; N, 6.77. Found: C, 45.19; H, 2.03; N, 6.55.

**Preparation of  $\{[\text{Mo}_2(\text{DmCF}_3\text{F})_3]_2(\mu_4\text{-C}_4\text{O}_4)\}\text{SbF}_6$ , **3**.** A mixture of **2** (248 mg, 0.100 mmol) and  $\text{NOSbF}_6$  (28.0 mg, 0.106 mmol) in 20 mL of  $\text{CH}_2\text{Cl}_2$  was allowed to stand undisturbed for about 1 week. This produced crystals that were essentially black. The crystalline product, obtained by decanting the solvent, was washed with isomeric hexanes, and dried under vacuum. Note: It was important to avoid stirring the reaction mixture to prevent formation of the product as a powder that decomposed during recrystallization attempts. Yield: 81 mg (30%). UV-vis in acetone,  $\lambda_{\text{max}}$  (nm) ( $\epsilon_{\text{M}}$ ,  $\text{M}^{-1} \text{cm}^{-1}$ ): 394 ( $5.2 \times 10^3$ ), 537 ( $1.6 \times 10^3$ ). Anal. Calcd for  $\text{C}_{94}\text{H}_{54}\text{F}_{42}\text{Mo}_4\text{N}_{12}\text{O}_4\text{Sb}$  (**3**): C, 41.52; H, 2.00; N, 6.18. Found: C, 41.19; H, 2.03; N, 6.10.

**Preparation of  $\{[\text{Mo}_2(\text{DAniF})_3]_2(\mu_4\text{-C}_4\text{O}_4)\}\text{(TFPB)}_2$ , **4**.** A mixture of **1** (104 mg, 0.0509 mmol) and  $[\text{Cp}_2\text{Fe}]\text{TFPB}$  (106 mg, 0.101 mmol) in  $\text{CH}_2\text{Cl}_2$  was stirred overnight before a mixture of isomeric hexanes (100 mL) was added to precipitate a dark-red product. After filtration, the solid was washed with 30 mL of isomeric hexanes and then dried under vacuum. Black crystals of the product were obtained from a  $\text{CH}_2\text{Cl}_2$  solution by layering with isomeric hexanes. Yield: 135 mg (70%). UV-vis in  $\text{CH}_2\text{Cl}_2$ ,  $\lambda_{\text{max}}$  (nm) ( $\epsilon_{\text{M}}$ ,  $\text{M}^{-1} \text{cm}^{-1}$ ): 416 ( $1.5 \times 10^3$ ), 487 ( $1.1 \times 10^4$ ). Anal. Calcd for  $\text{C}_{158}\text{H}_{114}\text{B}_2\text{F}_{48}\text{Mo}_4\text{N}_{12}\text{O}_{16}$  (**4**): C, 50.55; H, 3.06; N, 4.48. Found: C, 50.29; H, 3.10; N, 4.23.

**X-ray Structure Determinations.** Data were collected on a Bruker SMART 1000 CCD area detector system. Cell parameters were determined using the program SMART.<sup>49</sup> Data reduction and integration were performed with the software SAINT.<sup>50</sup> Absorption corrections were applied by using the program SADABS.<sup>51</sup> The positions of the Mo atoms were found via direct methods using the program SHELXTL.<sup>52</sup> Subsequent cycles of least-squares refinement followed by difference Fourier syntheses revealed the positions of the remaining non-hydrogen atoms. Hydrogen atoms

were added in idealized positions. All hydrogen atoms were included in the structure factor calculations. All non-hydrogen atoms, except those from disordered  $\text{CF}_3$  groups and solvent molecules, were refined with anisotropic displacement parameters. In **2**, **3**, and **4**, most of the  $\text{CF}_3$  groups are disordered over two or more orientations. Data collection and refinement parameters for **1–4** are summarized in Table 5. The core structures of these compounds are presented in Figure 1. Selected bond distances and angles are listed in Table 1.

**Computational Details.** DFT<sup>53</sup> calculations were performed with the hybrid Becke<sup>54</sup> three-parameter exchange functional and the Lee–Yang–Parr<sup>55</sup> nonlocal correlation functional (B3LYP) in the Gaussian 03 program.<sup>56</sup> Double- $\zeta$  quality basis sets (D95)<sup>57</sup> were used on C, N, and H atoms as implemented in Gaussian. Correlation-consistent double- $\zeta$  basis sets (CC-PVDZ)<sup>58</sup> were applied for the O atoms. A small effective core potential (ECP) representing the  $1s2s2p3s3p3d$  core was used for the molybdenum atoms along with its corresponding double- $\zeta$  basis set (LANL2DZ).<sup>59</sup> All calculations were performed on either Origin 3800 64-processor SGI or Origin 2000 32-processor SGI supercomputers located at the Texas A&M supercomputing facility.

**Acknowledgment.** We thank the Robert A. Welch Foundation, the National Science Foundation (IR/D program) and Texas A&M University for financial support. We also thank Dr. Dino Villagrán for helpful discussion on DFT calculations. We are grateful to the Laboratory for Molecular Simulation at TAMU for hardware and software and the TAMU supercomputer facility.

**Supporting Information Available:** X-ray crystallographic data for **1**· $3\text{CH}_2\text{Cl}_2$ , **2**· $1.5\text{C}_2\text{H}_5\text{OH}$ · $0.5\text{CH}_2\text{Cl}_2$ , **3**· $3\text{CH}_2\text{Cl}_2$ , and **4**· $3.5\text{CH}_2\text{Cl}_2$ · $0.5\text{C}_6\text{H}_{14}$  in standard CIF format. This material is available free of charge via the Internet at <http://pubs.acs.org>.

IC701937C

- (49) SMART for Windows NT, version 5.618; Bruker Advanced X-ray Solutions, Inc.: Madison, WI, 2001.  
 (50) SAINT Data Reduction Software, Version 6.36A; Bruker Advanced X-ray Solutions, Inc.: Madison, WI, 2001.  
 (51) SADABS Area Detector Absorption and other Corrections Software, Version 2.05; Bruker Advanced X-ray Solutions, Inc.: Madison, WI, 2001.  
 (52) Sheldrick, G. M. SHELXTL, version 6.12; Bruker Advanced X-ray Solutions, Inc.: Madison, WI, 2002.

- (53) (a) Hohenberg, P.; Kohn, W. *Phys. Rev.* **1964**, *136*, B864. (b) Parr, R. G.; Yang, W. *Density-Functional Theory of Atoms and Molecules*; Oxford University Press: Oxford, 1989.  
 (54) (a) Becke, A. D. *Phys. Rev. A* **1988**, *38*, 3098. (b) Becke, A. D. *J. Chem. Phys.* **1993**, *98*, 1372. (c) Becke, A. D. *J. Chem. Phys.* **1993**, *98*, 5648.  
 (55) Lee, C. T.; Yang, W. T.; Parr, R. G. *Phys. Rev. B* **1998**, *37*, 785.  
 (56) Frisch, M. J.; Trucks, G. W.; Schlegel, H. B.; Scuseria, G. E.; Robb, M. A.; Cheeseman, J. R.; Montgomery, J. A., Jr.; Vreven, T.; Kudin, K. N.; Burant, J. C.; Millam, J. M.; Iyengar, S. S.; Tomasi, J.; Barone, V.; Mennucci, B.; Cossi, M.; Scalmani, G.; Rega, N.; Petersson, G. A.; Nakatsuji, H.; Hada, M.; Ehara, M.; Toyota, K.; Fukuda, R.; Hasegawa, J.; Ishida, M.; Nakajima, T.; Honda, Y.; Kitao, O.; Nakai, H.; Klene, M.; Li, X.; Knox, J. E.; Hratchian, H. P.; Cross, J. B.; Bakken, V.; Adamo, C.; Jaramillo, J.; Gomperts, R.; Stratmann, R. E.; Yazyev, O.; Austin, A. J.; Cammi, R.; Pomelli, C.; Ochterski, J. W.; Ayala, P. Y.; Morokuma, K.; Voth, G. A.; Salvador, P.; Dannenberg, J. J.; Zakrzewski, V. G.; Dapprich, S.; Daniels, A. D.; Strain, M. C.; Farkas, O.; Malick, D. K.; Rabuck, A. D.; Raghavachari, K.; Foresman, J. B.; Ortiz, J. V.; Cui, Q.; Baboul, A. G.; Clifford, S.; Cioslowski, J.; Stefanov, B. B.; Liu, G.; Liashenko, A.; Piskorz, P.; Komaromi, I.; Martin, R. L.; Fox, D. J.; Keith, T.; Al-Laham, M. A.; Peng, C. Y.; Nanayakkara, A.; Challacombe, M.; Gill, P. M. W.; Johnson, B.; Chen, W.; Wong, M. W.; Gonzalez, C.; Pople, J. A. *Gaussian 03*, revision C.02; Gaussian, Inc.: Wallingford, CT, 2004.  
 (57) (a) Dunning, T. H.; Hay, P. J. In *Modern Theoretical Chemistry. 3. Methods of Electronic Structure Theory*; Schaefer, H. F., III, Ed.; Plenum Press: New York, 1977; pp 1–28. (b) Woon, D. E.; Dunning, T. H. *J. Chem. Phys.* **1993**, *98*, 1358.  
 (58) (a) Dunning, T. H. *J. Chem. Phys.* **1989**, *90*, 1007. (b) Woon, D. E.; Dunning, T. H. *J. Chem. Phys.* **1993**, *98*, 1358. (c) Wilson, A. K.; Woon, D. E.; Peterson, K. A.; Dunning, T. H. *J. Chem. Phys.* **1999**, *110*, 7667.  
 (59) (a) Wadt, W. R.; Hay, P. J. *J. Chem. Phys.* **1985**, *82*, 284. (b) Hay, P. J.; Wadt, W. R. *J. Chem. Phys.* **1985**, *82*, 299.